PHYSICAL REVIEW D **93,** 103517 (2016)

Limits on dark matter from AMS-02 antiproton and positron fraction data

Bo-Qiang Lu[1,2] and Hong-Shi Zong[1]
[1]*School of Physics, Nanjing University, Nanjing 210093, China*
[2]*Key Laboratory of Dark Matter and Space Astronomy, Purple Mountain Observatory, Chinese Academy of Sciences, Nanjing 210008, China*
(Received 28 October 2015; published 18 May 2016)

Herein we derive limits on dark matter annihilation cross section and lifetime using measurements of the AMS-02 antiproton ratio and positron fraction data. In deriving the limits, we consider the scenario of secondary particles accelerated in supernova remnants (SNRs), which has been argued to be able to reasonably account for the AMS-02 high-energy positron/antiproton fraction/ratio data. We parametrize the contribution of secondary particles accelerated in SNRs and then fit the observational data within the conventional cosmic ray propagation model by adopting the GALPROP code. We use the likelihood ratio test to determine the 95% confidence level upper limits of possible dark matter (DM) contribution to the antiproton/positron fractions measured by AMS-02. Under the assumption taken in this work, we find that our limits are stronger than that set by the Fermi-LAT gamma ray Pass 8 data observation on the dwarf spheroidal satellite galaxies. We show that the solar modulation (cosmic ray propagation) parameters can play a non-negligible role in modifying the constraints on dark matter annihilation cross section and lifetime for $m_\chi < 100$ GeV ($m_\chi > 100$ GeV), where m_χ is the rest mass of dark matter particles. We also find that constrains on DM parameters from AMS-02 data would become more stringent when the solar modulation is weak. Using these results, we also put limits on the effective field theory of dark matter.

DOI: 10.1103/PhysRevD.93.103517

I. INTRODUCTION

Eighty years after the discovery of dark matter (DM) [1–6], the nature of dark matter still remains mysterious. Among various hypothetical particles, the so-called weakly interacting massive particle (WIMP) is the leading candidate [7–11]. It is also widely believed that WIMPs could annihilate one another and then generate (or alternatively decay into) stable particles, such as high energy gamma-rays and pairs of electrons/positrons, protons/antiprotons, and neutrinos/antineutrinos [10,11]. Such particles propagate into the Galaxy and become part of cosmic rays (CRs). The accurate measurements of cosmic rays hence in turn provide people a valuable chance to study dark matter particles indirectly. The indirect detection of dark matter particles with space-based cosmic ray detectors has been a quickly evolving field since 2008 [12–18]. The most extensively discussed signature is the high energy spectra of cosmic ray electrons and positrons (equally, the positron to electron ratio data) that are well in excess of the prediction of the conventional cosmic ray propagation model, i.e., the so-called electron/positron excesses [19]. Before 2015, due to lack of evidence for an antiproton excess [20], the electron/positron excesses have been widely attributed to the leptonic dark matter annihilation/decay [21–26]. Nevertheless, the astrophysical origins, such as electron/positron pairs from pulsars [27] or the secondary/primary particles accelerated in the SNRs [28–35], can also reasonably account for the data. In the PAMELA era, in view of lack of distinct spectral structures that are predicted to arise in dark matter annihilations/decays into electrons/positrons in the data, some researchers constrained the physical parameters of these exotic particles by assuming that the positron fraction excess arises from a group of pulsars [24]. With the first AMS-02 result (i.e., the positron fraction up to ~350 GeV [15]), assuming that the positron fraction excess is mainly contributed by astrophysical processes and using the same phenomenological parametrization as the AMS Collaboration in their analysis, Bergström *et al.* obtained very stringent limits on dark matter annihilating or decaying to leptonic final states [36]. Later, the positron flux data or alternatively the electron flux data has been adopted to set limits on dark matter annihilation/decay channels [37,38]. Recently, the AMS-02 antiproton-to-proton ratio data has been announced in a dedicated conference [39] and the high energy part seems to be in excess of the regular prediction of conventional cosmic ray propagation model (while in Refs. [40,41], they argued that the background was enough to explain AMS-02 antiproton data if uncertainties in propagation model, solar modulation and nucleon collision process were taken into account). In this work we take both the antiproton ratio data and the positron fraction data to place limits on the physical parameters of dark matter particles. The pulsar model may account for the positron fraction excess but may not for the antiproton data. Herein we consider the scenario of secondary particles accelerated in SNRs [28,29] which may simultaneously explain both the positron fraction and antiproton ratio observed by AMS-02 experiment.

 © 2016 American Physical Society

Following the phenomenological AMS parametrization approach we parametrize the contribution of the SNR with a simple function and calculate the background (BKG) ratio of positron and antiproton with GALPROP [42], then we add the SNR component to the BKG component as the total ratio at the top of the atmosphere (TOA). Constraints on the dark matter annihilation cross section and lifetime are placed with these results, and we find that the limits obtained by means of such a method are stronger than the limits given by Ackermann *et al.* [43], which derived from Fermi-LAT gamma-ray Pass 8 data observation on the dwarf spheroidal satellite galaxies. Further more, we also use these results to put constraints on the effective field theory which is mostly discussed at direct detection and Large Hadron Collider (LHC).

This work is arranged as the following. In Sec. II we briefly introduce a possible origin of cosmic ray, the model of secondary particle acceleration in SNR and some details of BKG CR propagation model. In Sec. III we present our limits on dark matter parameters and study the uncertainties caused by propagation parameters, solar modulation parameters and dark matter distribution profile models. And in Sec. IV we put limits on the effective field theory by using the results we obtain in Sec. III. We summarize our results in Sec. V.

II. THE ASTROPHYSICAL ORIGIN MODEL OF AMS-02 ANTIPROTON RATIO AND POSITRON FRACTION DATA

A. The origin of cosmic ray

It is widely known that the source of energy up to ∼PeV for cosmic rays acceleration is thought to be shock waves driven by the expanding ejecta of supernovae (SNe) [44,45]. However, the origin of cosmic rays is still only partially understood. From the measurements of isotopic composition of the galactic cosmic ray (GCR) beryllium, it shows that the CRs lifetime for escape is $\sim 1.7 \times 10^7$ years and the average density through which CRs have traveled is ~ 0.2 atms cm^{-3} while the interstellar density of the Galactic disk is ~ 1 atm cm^{-3}. One of the solutions to the observations was suggested by Kafatos *et al.* [46] that cosmic rays might be accelerated in superbubbles formed by OB associations. Such a scenario is supported by many isotopic ratio experiment observations. For example, Cassé and Paul [47] suggested that the large ^{22}Ne/^{20}Ne ratio in GCRs observed by Voyager [48], Ulysses [49] and CRIS [50,51] could be due to Wolf-Rayet star (WR star) ejecta mixing with material of solar system composition. This hypothesis also predicts an excess of the elemental Ne/He ratio, which has been confirmed observationally. Binns *et al.* [50–52] show that other observations data of isotopic ratio such as ^{12}C/^{16}O, ^{14}N/^{16}O, N/Ne, and ^{58}Fe/^{56}Fe can be well explained by the WR star model. Further evidence of superbubble origin comes from measurements of the ^{59}Ni and ^{59}Co isotopes' abundance. Cassé *et al.* [53] pointed out that radioactive nuclide that are produced in supernova explosions can decay only by electron capture, as nuclei are accelerated to GCR energies, orbital electrons are quickly stripped off and nuclei that decay only by electron capture become stable, which can be used to distinguish between models involving long and short time delays between nucleosynthesis and acceleration. The CRIS measurements of ^{59}Ni and ^{59}Co isotopes [54] show that the ^{59}Ni in GCRs has completely decayed, which leads us to conclude that refractory GCRs must reside in an atomic or molecular state, most likely in interstellar grains, for a time $\gtrsim 10^5$ yr before acceleration to GCR energies [51,54]. This conclusion also supports the scenario that GCRs are being accelerated from dust and gas within superbubbles. The mean time between SN events within superbubbles is estimated to be $\sim 3 \times 10^5$ yr [55], and shocks from SNe within the superbubble occur on an average time scale $> 10^5$ yr, thus providing sufficient time for ^{59}Ni to decay to ^{59}Co [54]. However, superbubbles cannot be the entire solution to the origin of GCRs. For instance, superbubbles can neither account for the low large-scale anisotropy of CRs nor explain the shallow CR gradient deduced from gamma ray data [56].

In the standard CR model, primary CRs are released into interstellar space after accelerated in supernova remnants (SNRs) sources, the secondary CRs such as positron, antiproton and boron are produced by the interaction of primaries with ISM during their propagation [57]. The source spectrum of primary CRs has a power law behavior i.e. $Q_{\rm inj}(E) \propto E^{-\gamma}$, which naturally arises from diffusive shock acceleration. In the Following, we assume that the injected spectrum of proton and electron has the power law form $Q^{\rm p}_{\rm inj} \propto E^{-\gamma_{\rm p}}$, $Q^{\rm e^-}_{\rm inj} \propto E^{-\gamma_{\rm e^-}}$. The reacceleration and convection effects can be ignored at sufficiently high energies, thus we can use the leaky-box model to describe the propagation of CRs. Under the leaky-box model, the observed primary spectrum is estimated to be $N_{\rm obs}(E) \propto Q_{\rm inj}(E)\tau_{\rm esc} \propto E^{-\gamma-\delta}$, where $\tau_{\rm esc} \propto E^{-\delta}$ is the escape time from the Galaxy, with $\delta \sim 0.3$–0.6. In the standard model secondaries mainly arise as the products of protons interact with ISM in the Galaxy, thus the injected spectrum of secondary is $Q_{\rm sec}(E) \propto E^{-\gamma_{\rm p}-\delta}$ [58]. After the production of the secondaries, they suffer nearly the same effects of propagation (mainly diffusion and energy losses of leptons at sufficiently high energies we concern here) in the Galaxy as the primaries, thus such effects cancel out each other in secondary-to-primary ratio. We come to the conclusion that the leaky-box model predicts a power law form for the secondary-to-primary ratio reading, $\mathcal{R}_{\rm LBM} \propto E^{-\delta}$. For the case of positron fraction $\mathcal{R}^{e^+}_{\rm LBM} \propto E^{-\gamma_{\rm p}-\delta+\gamma_{\rm e^-}}$, we note that the fits to the AMS-02 electron and proton data indicate $\gamma_{\rm e^-} \simeq 2.6$ [37] and $\gamma_{\rm p} \simeq 2.4$ [59] which means $-\gamma_{\rm p} - \delta + \gamma_{\rm e^-} \lesssim 0$ (see the BKG component of positron fraction in the

upper right panel of Fig. 1), thus the positron fraction also decreases with energy at high energies in the standard CR model. However, the fits to the AMS-02 antiproton ratio and positron fraction data indicate $\mathcal{R}^{\bar{p}}_{\rm DAT} \sim 2.0 \times 10^{-4}$ and $\mathcal{R}^{e+}_{\rm DAT} \propto E^{1.0}$ at energy above ~10 GeV. Nondetection of the softening in positron fraction and antiproton ratio at high energies suggests a deviation of standard CR model. After PAMELA published the "abnormal" positron fraction data, the pulsars were considered to be powerful sources of electrons and positrons in the Galaxy. It is believed that lepton pairs can be generated from the rotating electromagnetic field of the pulsar and then the termination shock from supernova accelerates the incoming pairs to very high energies. After acceleration, these particles are trapped in pulsar wind nebula magnetic field for a long time (~50 kyr) before they are released into ISM [60]. While such a scenario may account for positron fraction observed by PAMELA and AMS-02, it cannot explain the constant antiproton ratio at energies ~10–300 GeV observed by AMS-02. From the viewpoint of diffusive shock acceleration mechanism, a constant or even an increasing ratio of secondary-to-primary CRs indicates that the secondaries are accelerated in the same region as primaries. In this work, we make use of the scenario which is pointed out by Blasi *et al.* [28–31] that the secondary CRs (positron and antiproton) can also be produced and accelerated in SNR source. In this scenario, the "excesses" in positron and antiproton are due to the secondary products of hadronic interactions inside SNRs. The dense environment and old SNRs are the most important ingredients for the production of positron and antiproton, and the crucial physical process which leads to a natural explanation of the positron and antiproton flux is the fact that the secondary production takes place in the same region where primary CRs are being accelerated [29]. In such a scenario, one can naturally explain the AMS-02 positron fraction and antiproton ratio simultaneously while in no need of any new class of source such as DM or pulsars. As is shown in Ref. [56], the direct spectral signatures of GCR acceleration may have been seen in many older SNRs, such as IC 443, W28, G353.6-0.7 and perhaps W41. Following the Refs. [28,31] the evolution of the gyrophase and pitch angle averaged phase space density $f_{\rm i} \equiv f_{\rm i}(x,p)$ of species i is governed by the transport equation

$$\frac{\partial f_{\rm i}}{\partial t} = -u\frac{\partial f_{\rm i}}{\partial x} + \frac{\partial}{\partial x}D_{\rm i}\frac{\partial f_{\rm i}}{\partial x} - \frac{p}{3}\frac{du}{dx}\frac{\partial f_{\rm i}}{\partial p} + Q_{\rm i}(x,p), \quad (1)$$

and the solution of this equation is found to be

$$f_{\rm i}(x=0,p) = \gamma\left(\frac{1}{\xi}+r^2\right)\int_0^{\rm p}\frac{dp'}{p'}\left(\frac{p'}{p}\right)^{\gamma}\frac{D_{\rm i}(p')}{u_-^2}Q_{\rm i}(p'), \quad (2)$$

where $-$ represents upstream and $+$ represents downstream, the slope $\gamma = 3u_-/(u_- - u_+) = 3r/(r-1)$, u is the velocity of fluid, $r = u_-/u_+$ is the compression factor. For a strong shock $r \to 4$ and $\gamma \to 4$. The factor ξ represents the mean fraction of energy of an accelerated proton carried away by a secondary particle in each scattering. $D_{\rm i}(p) \propto p^{\alpha}$ is the diffusion coefficient of the shock [28]. The production rate at a position x around the shock is

$$Q_{\rm i}(x,E) = \sum_{\rm j}\int d\sigma_{\rm ji}(E',E)cN_{\rm j}(x,E')n_{\rm gas}(x), \quad (3)$$

where c is the speed of light, $\sigma_{\rm ji}(E',E)$ is the cross section for a primary specie j of energy E' to produce a secondary particle i of energy E. $n_{\rm gas}$ is the gas density in the shock region. The efficiency of secondary CR nuclei production in SNRs depends significantly on the density of ISM in which SNRs are exploding [61,62]. The source spectrum $N_{\rm j} = 4\pi p^2 f_{\rm j}(p)u_+\tau_{SN}$ and $f_{\rm j} \sim p^{-\gamma}$ then $N_{\rm j} \sim p^{-\gamma+2}$. Then one can find that $f_{\rm i}(x=0,p) \sim p^{-\gamma+\alpha}$ and $\alpha > 0$ is the slope of the diffusion coefficient (in the following α is taken as 1 for a Bohm-like diffusion coefficient). This result indicates that the equilibrium spectrum of the particles that take part in the acceleration is flatter than the injection spectrum of secondary particles [28,31]. As is presented in [29] the observed secondary-to-primary ratio (such as $\bar{p}/p$) which contributes from accelerating in SNRs can be easily derived with above results

$$\mathcal{R}_{\rm SNR}(E) \simeq cn_{\rm gas}[\mathcal{A}(E) + \mathcal{B}(E)], \quad (4)$$

where

$$\mathcal{A}(E) = \gamma(1/\xi + r^2)\int_m^E dy y^{\gamma-3}\frac{D_-(y)}{u_-^2} \times \int_y^{E_{\rm max}} dz z^{2-\gamma}\sigma_{\rm ji}(z,y), \quad (5)$$

and

$$\mathcal{B}(E) = \frac{\tau_{\rm SN} r}{2E^{2-\gamma}}\int_E^{E_{\rm max}} dz z^{2-\gamma}\sigma_{\rm ji}(z,E). \quad (6)$$

One can easily find that $\mathcal{B}(E)$ term is nearly a small constant and has been neglected in this work, and $\mathcal{A}(E) \propto E^{-\kappa^{\alpha}+2}$, where κ^{α} is a factor that is determined by nuclear collision process. These simplifications show that the slope of observed secondary-to-primary ratio that contributes from accelerating in SNRs does not depend on the accelerating process but is mainly dominated by the collision processes of CRs. We notice that the Eq. (4) is also suitable for the case of positron

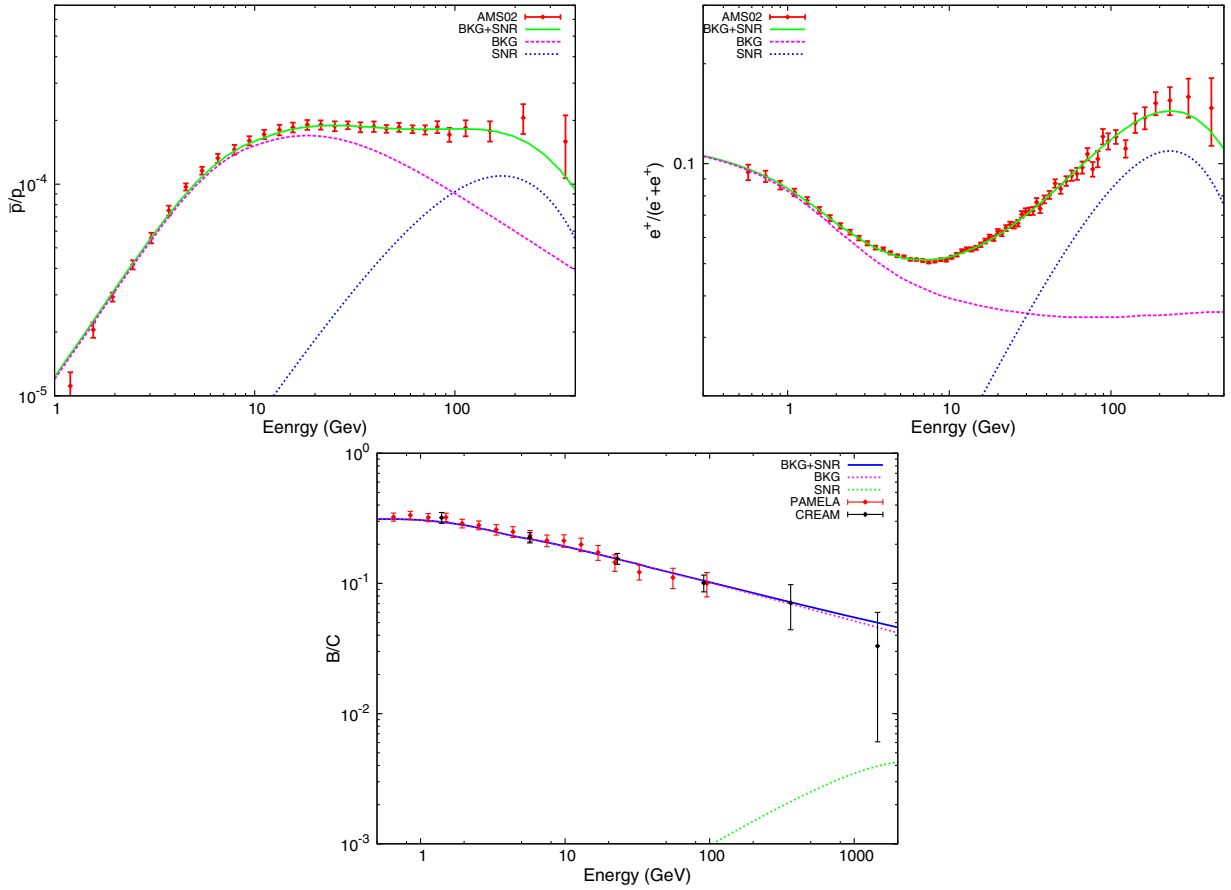

FIG. 1. Upper left panel: fit to the AMS-02 antiproton ratio with BKG component and SNR component. Upper right panel: fit to the AMS-02 positron fraction data with BKG component and SNR component. Lower panel: fit to PAMELA and CREAM B/C data.

fraction, the reason is that since positrons and electrons suffer nearly the same energy loss after being released into the interstellar space, so the energy losses of positrons and electrons cancel out each other in positron fraction. This conclusion may be seen from the BKG component of positron fraction in the upper right panel of Fig. 1. Spallation and decay are taken into account in [30,31] [add a term $-\Gamma_i f_i$ on the right hand of Eq. (1)] which lead to a suppression of the secondary contribution at very high energies. In this work we take a form of the contribution to the observed secondary-to-primary ratio from SNRs as

$$\mathcal{R}^{\alpha}_{\rm SNR}(E) = \mathcal{N}^{\alpha}_{\rm SNR}(E/1\ {\rm GeV})^{-\kappa^{\alpha}+2}\exp(-E/E^{\alpha}_{\rm c}), \quad (7)$$

where α stands for different kinds of secondary CRs, $\mathcal{N}^{\alpha}_{\rm SNR}$ is a normalized coefficient and $E^{\alpha}_{\rm c}$ is the cutoff energy. Thus the observed ratio of secondary-to-primary at TOA is given by $\mathcal{R}^{\alpha}_{\rm TOA} = \mathcal{R}^{\alpha}_{\rm BKG} + \mathcal{R}^{\alpha}_{\rm SNR}$.

B. Cosmic ray propagation model

The propagation of CRs in the Galaxy is described by the transport equation [63,64]

$$\frac{\partial\psi}{\partial t} = \nabla\cdot(D_{\rm xx}\nabla\psi - V_{\rm c}\psi) + \frac{\partial}{\partial p}p^2 D_{\rm pp}\frac{\partial}{\partial p}\frac{1}{p^2}\psi - \frac{\partial}{\partial p}\left[\dot{p}\psi - \tfrac{p}{3}(\nabla\cdot V_{\rm c}\psi)\right] - \frac{\psi}{\tau_{\rm f}} - \frac{\psi}{\tau_{\rm r}} + Q(x,p), \quad (8)$$

where $\psi(\vec{r},p,t)$ is the CR density per unit of total particle momentum p at position $\vec{r}$ and $D_{\rm xx}$ is the spatial diffusion coefficient that can be parametrized as $D_{\rm xx} = D_0\beta(R/R_0)^{\delta}$, where $\beta = v/c$ and $R = pc/Ze$ is the particle rigidity. We use the default setting of propagation parameters in the GALPROP: $D_0 = 5.3\times10^{28}({\rm cm^2\,s^{-1}})$, $R_0 = 4.0$ GV and $\delta = 0.33$. With such propagation values the B/C and ^{10}Be/^{9}Be observed by PAMELA and other experiments can be well explained. However, there exist degeneracies of different set of propagation parameters, which cannot be distinguished with present experiments, so we also consider the effect of the propagation parameters on our limit results in the following. $D_{\rm pp}$ is diffusion coefficient in the momentum space and is related to $D_{\rm xx}$ by

$$D_{\rm pp}D_{\rm xx} = \frac{4p^2v_A^2}{3\delta(4-\delta^2)(4-\delta)\omega}, \quad (9)$$

where ω characterizes the level of turbulence and is taken as 1, and v_A is Alfvén speed which is set at 33.5 km s^{-1} in the diffusion reacceleration (DR) scheme. V_c is the convection velocity that is assumed to increase linearly with distance from the plane [63,65], $\nabla \cdot V_c$ represents adiabatic momentum gain or loss in the nonuniform flow of gas with a frozen-in magnetic field whose inhomogeneity scatters the CRs [64], $\dot{p} = dp/dt$ is the momentum gain or loss rate, and τ_r and τ_f are characteristic time scales for radioactive decay and loss by fragmentation. $Q(x, p)$ is the source term including primary, spallation and decay contributions. The distribution of CR sources is taken as [63]

$$q(r,z) = q_0 \left(\frac{r}{r_\odot}\right)^\eta \exp\left(-\xi \frac{r - r_\odot}{r_\odot} - \frac{|z|}{0.2\ \text{kpc}}\right), \quad (10)$$

where q_0 is a normalization constant, $r_\odot = 8.5$ kpc is the solar position in the Galaxy, η and ξ are the source distribution parameters, which are determined by fitting to the observation of gamma-ray data [42,63,64], z is the column height of the Galaxy and its maximum value is set at $z_h = 4$ kpc [42], but as is shown in the upper left panel of Fig. 4, our limit results are not sensitive to z_h, and r is the Galaxy radius and a cutoff had been used in the source distribution at $r = 20$ kpc since it is unlikely that significant sources are present at such large radii [63,64]. The DR propagation model has been adopted in this work.

We point out that the BKG component, like SNR component, can also be obtained by using phenomenological AMS parametrization approach [36], or on the other hand the propagation of the SNR component (secondary particle accelerated in SNRs as a source) can also be calculated by using GALPROP (and a nice fit results of positron fraction and antiproton ratio can be found in Ref. [31]). The former is a fully parametrization method and the latter is a fully physical method, while the limits on DM parameters do not change significantly between these two methods [36] because the ratio (or flux) at TOA is nearly the same for the two methods (see also in Refs. [36,37] for a justification of this approach). The aim of our method presented in this work is to obtain the right ratio or fraction at TOA and to provide a physical interpretation for our parametrization approach at the same time. In the lower panel of Fig. 1 we show the fits to B/C ratio observed by PAMELA [66] and CREAM [67] experiments with the propagation parameters that we give in this section. The χ^2/DOF is 11/20 and the fit results of ($\mathcal{N}^B_{SNR}$, κ^B, E^B_c) are (5.0×10^{-5}, 0.65, 4.0×10^3 GeV). Thus, the observation of B/C ratio is consistent with standard CR model up to ~1 TeV, which puts stringent limits on the SNR acceleration model. References [32,33] propose a two-component SNR acceleration scenario where the secondary CRs are contributed from a set of nearby old SNRs, and high-energy part of the CR flux is provided by a galactic ensemble of SNRs. Under such a scenario, the primary CRs and the CR ratios such as $e^+/(e^- + e^+)$, $\bar{p}/p$, and B/C can be well accounted for simultaneously. In essence, our assumption in this work is that the "excesses" in positron fraction and antiproton ratio observed by AMS-02 are astrophysical origin, and the realization of the hypothesis is represented by a phenomenological parametrization approach given by Eq. (7), with three free parameters ($\mathcal{N}^\alpha_{SNR}$, κ^α, E^α_c). The B/C ratio can also be well fitted by this method, with a relatively small normalized coefficient $\mathcal{N}^\alpha_{SNR}$. From the viewpoint of two-component SNR acceleration scenario, a small normalization coefficient is due to a suppression in B/C ratio that contributes from the Galactic SNRs. We emphasize that the association between the SNR acceleration scenario and the approach presented here is not necessary. The SNR acceleration scenario provides us an attractive physical interpretation of the astrophysical origin but whether this scenario is reasonable or not needs further tests.

III. LIMITS ON THE DARK MATTER PARAMETERS

We consider the DM annihilation or decay into the following channels

$$\chi\bar{\chi} \to b\bar{b}, u\bar{u}, W^+W^-, \mu^+\mu^-, \tau^+\tau^- (\text{annihilation}),$$

$$\chi \to b\bar{b}, u\bar{u}, W^+W^-, \mu^+\mu^-, \tau^+\tau^- (\text{decay}),$$

each with 100% branching ratio. The annihilation or decay of dark matter particles in the Milky Way dark matter halo at the position $\vec{r}$ with respect to the Galactic center produce a primary flux with a rate (per unit energy and unit volume) that is given by [68]

$$Q_{\text{anni}}(\vec{r}, E) = \frac{\langle \sigma v \rangle}{2m_\chi^2} \frac{dN}{dE} \times \rho_\chi^2(\vec{r}), \quad (11)$$

$$Q_{\text{decay}}(\vec{r}, E) = \frac{1}{\tau m_\chi} \frac{dN}{dE} \times \rho_\chi(\vec{r}), \quad (12)$$

where m_χ is DM mass, τ is DM particle lifetime, $\langle \sigma v \rangle$ is DM velocity-weighted annihilation cross section, dN/dE is the energy spectrum of SM particles produced in the annihilation or decay of DM particles which we simulate by using the event generator PYTHIA package [69], and ρ_χ is the density of dark matter particles in the Milky Way halo. We note that the prediction of CR flux originated from DM annihilation or decay crucially depends on the density distribution of DM in the Galactic halo; however, the astrophysical uncertainty from the DM profile distribution is irreducible presently. In this work the profile is adopted to be Navarro-Frenk-White (NFW) distribution [70] and Einasto and Isothermal distributions are also taken as a comparison. The NFW DM distribution profile in the Galactic halo is read as

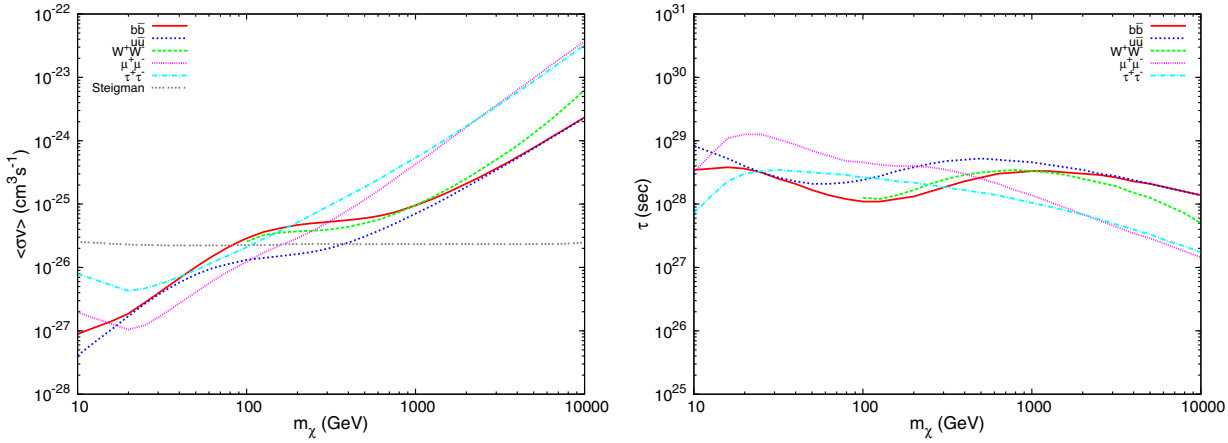

FIG. 2. Left panel: limits on the DM annihilation cross section at 95% C.L. derived from the AMS-02 data. The gray curve in this and subsequent figures corresponds to the thermal relic cross section adopted from Steigman *et al.* [75]. Right panel: limits on the DM annihilation cross section at 95% C.L. derived from the AMS-02 data. The positron fraction is used to calculate the limits for the final states $\mu^+\mu^-$ and $\tau^+\tau^-$ while antiproton ratio is used to calculate the limits for the final states $b\bar{b}$, $u\bar{u}$ and W^+W^-.

$$\rho(r) = \frac{\rho_s}{(r/r_s)(1+r/r_s)^2}, \tag{13}$$

where $r_s = 20$ kpc and $\rho_s = 0.26\ \mathrm{GeV\,cm^{-3}}$. Such a value of ρ_s corresponds to a local DM energy density of $0.3\ \mathrm{GeV\,cm^{-3}}$ [22]. We notice that currently the more likely value is $0.43\ \mathrm{GeV\,cm^{-3}}$ [71]. Such a correction of course is minor but the limits would be tighter by a factor of 2 (annihilation model) or 1.4 (decay model). We notice here although under ΛCDM hypothesis large N-body numerical simulations lead to the commonly used NFW halo cuspy spatial density profile, analysis of observations in the central regions of various dwarf halos is in favor of cored profiles, which are much flatter than cusp profiles [72]. This problem may stem from ΛCDM hypothesis which assumes weak self-interactions and weak interactions with ordinary matter, and self-interaction DM scenario may provide one of the possible solutions to this problem [73]. One can estimate that such a change in the profile has an insignificant impact on leptons since energy losses dominate the propagation of leptons at high energies, and as is shown in the lower right panel of Fig. 4, limits on quark channels alter less than ∼10%–20% when changing the DM inner profile.

The statistical method of likelihood ratio test developed in [74] is adopted to put limits on a possible DM contribution to the data measured by AMS-02. The likelihood function $\mathcal{L}(\vec{\theta})$ is taken the form as

$$\mathcal{L}(\vec{\theta}) = \exp(-\chi^2(\vec{\theta})/2), \tag{14}$$

where $\vec{\theta} = \{\theta^1, \theta^2, \ldots, \theta^n\}$ is the parameters of the model, and the $\chi^2(\vec{\theta})$ function is

$$\chi^2(\vec{\theta}) = \sum_{\mathrm{i}}^{\mathrm{m}} \frac{(\lambda_{\mathrm{i}}^{\mathrm{exp}} - \lambda_{\mathrm{i}}^{\mathrm{the}})^2}{\sigma_{\mathrm{i}}^2}, \tag{15}$$

where m is the number of data, $\lambda_{\mathrm{i}}^{\mathrm{exp}}$ is the measured value and $\lambda_{\mathrm{i}}^{\mathrm{the}}$ is the theory value for a certain model and σ_{i} is the known deviation of measurement. For antiproton ratio, the χ^2/DOF is 22/24 and the fit results of $(\mathcal{N}_{\mathrm{SNR}}^{\bar{p}}, \kappa^{\bar{p}}, E_{\mathrm{c}}^{\bar{p}})$ are $(2.364 \times 10^{-7}, 0.540, 139.530\ \mathrm{GeV})$. For positron fraction, the χ^2/DOF is 43/58 and the fit results of $(\mathcal{N}_{\mathrm{SNR}}^{e^+}, \kappa^{e^+}, E_{\mathrm{c}}^{e^+})$ are $(1.440 \times 10^{-3}, 1.026, 238.062\ \mathrm{GeV})$. Upper limits at the 95% C.L. on the DM annihilation or decay rate are derived by increasing the signal normalization from its best-fit value of astrophysical source model we have discussed above until χ^2 changes by 2.71 i.e.

$$\chi^2_{\mathrm{DM}} = \chi^2 + 2.71. \tag{16}$$

Following this procedure, the positron fraction is used to calculate the constraints on the annihilation cross section and lifetime for the final states $\mu^+\mu^-$ and $\tau^+\tau^-$ while antiproton ratio is used to calculate the constraints on the annihilation cross section and lifetime for the final states $b\bar{b}$, $u\bar{u}$ and W^+W^-, the results are presented in Fig. 2. In the left panel of Fig. 3, we compare our results with the limits given by Ackermann *et al.* [43], which derived from Fermi-LAT gamma-ray Pass 8 data observation on the dwarf spheroidal satellite galaxies, we find that our limits are stronger than theirs both for the $\tau^+\tau^-$ and $b\bar{b}$ final states.

In the right panel of Fig. 3, we study the effect of solar modulation on our limit results. After entering into the solar system, the Galactic CRs are suffering to convection, particle drift and adiabatic energy loss in the interplanetary magnetic field carried out by the solar wind. Such an effect is the so-called solar modulation that depends, via drifts in

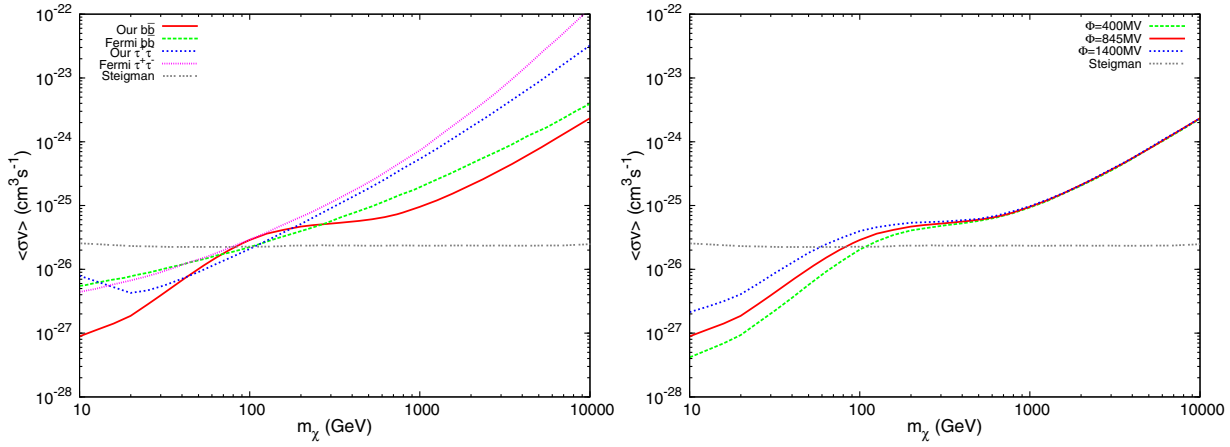

FIG. 3. Left panel: comparison of our results with the upper limits from the Fermi-LAT observations of dwarf galaxies. Right panel: the effect of the solar modulation parameter ϕ on the limit results.

the large-scale gradients of the solar magnetic field (SMF), on the particle charge including its sign. As a result, the solar modulation depends on the polarity of the SMF, which changes periodically every ∼11 years [76]. Recently the stochastic method is used to solve the four-dimensional Parker (1965) transport equation which describes the transport of charged particles in the solar system. Such progresses are remarkable; however, there are still some uncertainties in this theory and the code is time-consuming. So in this work we only use the force field approximation since it works well above about 0.5 GeV [77]. We consider the solar modulation uncertainty $\Delta\phi \simeq 200$ MV around the

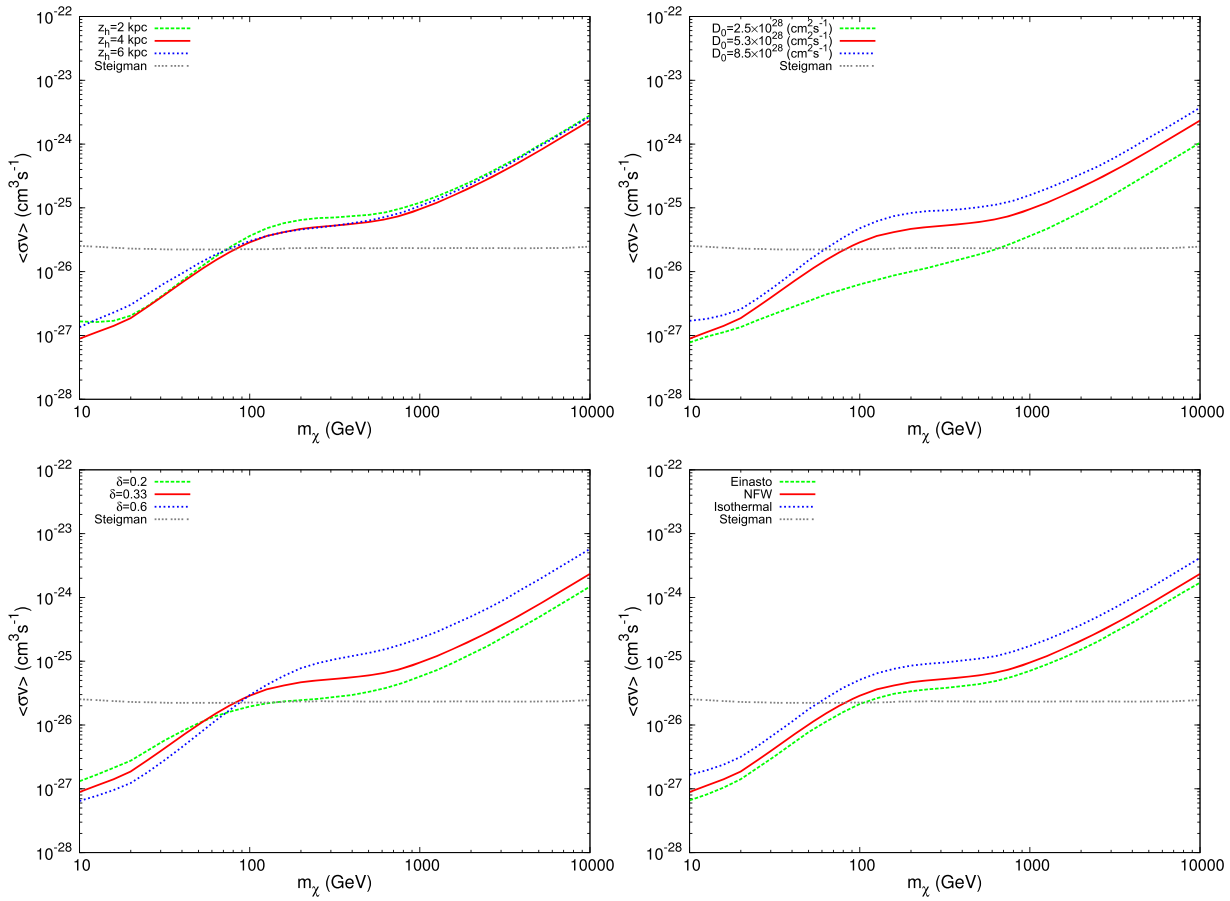

FIG. 4. Effects on the limit results with different propagation parameter and DM distribution profile.

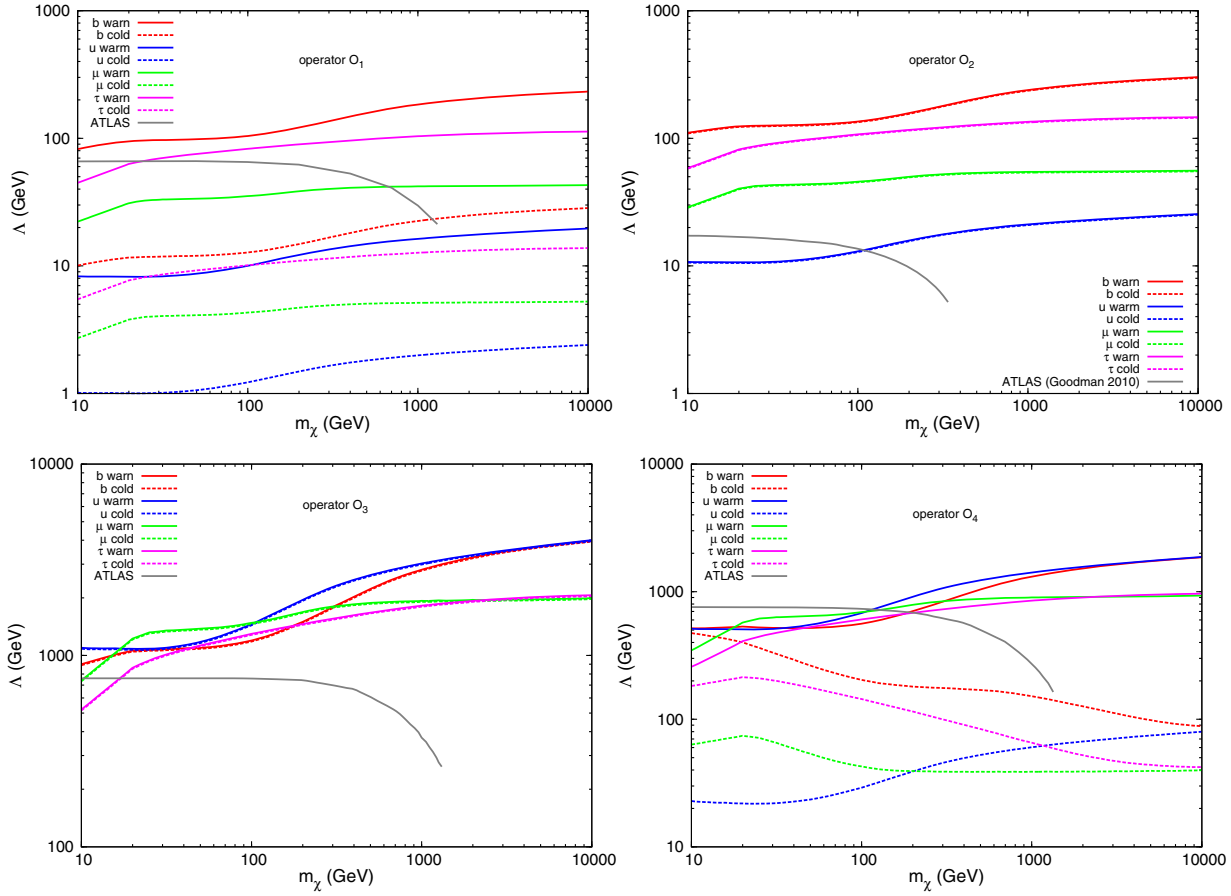

FIG. 5. Limits on Λ as a function of the DM particle mass m_χ at 95% C.L., for various operators as described in the texts. For each operator final state of b and u quarks, μ and τ leptons are calculated, and for each final state we consider the case of warm DM and cold DM respectively, the ATLAS results are from [78,80–82].

best-fit value $\phi = 845$ MV, as shown in the right panel of Fig. 3, the uncertainty has an utmost value about 16% at 10 GeV, then declines to zero at ∼300 GeV. The results shown in the right panel of Fig. 3 also indicate that constrains on DM parameters from AMS-02 data would become more stringent when the solar modulation is weak.

In Fig. 4 we study the effect of propagation parameters of z_h, D_0 and δ on our limit results (just the $b\bar{b}$ final state is considered because for the final states of $\mu^+\mu^-$ and $\tau^+\tau^-$ the results are found to be insensitive to the propagation parameters [38]). Specifically, each time we change one parameter, we fix the others to be fiducially values mentioned above. We find that the exclusion line alters slightly with the column height of the Galaxy z_h, so it may only contribute about 2% uncertainty of our results if the uncertainty $\Delta z_h \simeq 0.5$ kpc is taken into account. The situation changes significantly for the diffusion parameters D_0 and δ since the diffusion process dominates the propagation of antiprotons in the Galaxy. For example, with an uncertainty $\Delta D_0 \simeq 1.0 \times 10^{28}$ (cm^2 s^{-1}) in D_0, our limits changes ∼2% for $m_\chi \leq 30$ GeV but ∼16% for $m_\chi \sim$ 30–1000 GeV then declining to ∼10% above 1000 GeV. In the case of δ, if one considers the uncertainty $\Delta\delta \simeq 0.1$ in δ, then it contributes about 4% uncertainty for $m_\chi < 100$ GeV, while above 100 GeV the uncertainty rises to ∼14%. In the right bottom panel of Fig. 4 we study the effect of DM distribution profile on the limits, we can find that it contributes about 20% uncertainty in the whole DM mass range if we consider the NFW profile as the standard DM distribution profile. So the propagation parameters contribute most uncertainty at large DM mass (above ∼100 GeV) while the most uncertainty at low DM mass is contributed from solar modulation, since the diffusion dominates the propagation of CRs at high energy while the solar modulation affects the CRs mostly at lower energy. As a result, the uncertainty of the limits on the DM parameters is ∼20%–30% in the whole DM mass range if we take into account the contributions of propagation parameters and solar modulation, this value rises to ∼40%–50% if the contributions of DM distribution profile have been considered.

The other forms of uncertainty may contribute from the energy spectrum dN/dE which is generated from PYTHIA in this work. The degeneracy between diffusion reacceleration (DR) and diffusion convection (DC) propagation model may also contribute uncertainty to the limits results,

but this is tiny, specifically, for the final state $b\bar{b}$, $u\bar{u}$ and W^+W^- the diffusion dominates the propagation of antiproton, and for the final states $\mu^+\mu^-$ and $\tau^+\tau^-$ the difference of limit results between DR and DC will be little especially at $m_\chi > 200$ GeV [37] since energy losses dominate the propagation of leptons at high energies.

IV. CONSTRAINS ON THE EFFECTIVE FIELD THEORY

A. Dark matter annihilation

In the following, we use our results to put limits on parameters of effective field theory (EFT). We assume dark matter as a Dirac fermion (we note that in the above results we have assumed a self-conjugate DM particle, the limits will improve by a factor 2 for the Dirac fermion case). The WIMPs may interact with SM particles through a dark gauge sector, this symmetry is spontaneous breaking at low energy and leading to a suppression of the interaction between WIMPs and SM particles. The EFT can approximately describe such interaction by using higher-dimensional operators, and this method is model independent [78]. But we should bear in mind that this method will break down when the typical reaction energy is much higher than the mediator mass. In this work we study the following EFT operators

$$\mathcal{O}_1 = \frac{m_f}{\Lambda^3}\bar{\chi}\chi\bar{f}f$$
$$\mathcal{O}_2 = \frac{m_f}{\Lambda^3}\bar{\chi}\gamma_5\chi\bar{f}\gamma_5 f$$
$$\mathcal{O}_3 = \frac{1}{\Lambda^2}\bar{\chi}\gamma_\mu\chi\bar{f}\gamma^\mu f$$
$$\mathcal{O}_4 = \frac{1}{\Lambda^2}\bar{\chi}\gamma_\mu\gamma_5\chi\bar{f}\gamma^\mu\gamma_5 f,$$

where f is a SM fermion and m_f is the mass, $\Lambda = \frac{M}{g_\chi g_f}$, M is the mass of the exchanged particle, g_χ and g_f are the couplings. Then the annihilation cross sections of the operators are given by [79]

$$\langle\sigma_1 v\rangle = \frac{N_c m_f^2}{8\pi\Lambda^6}\sqrt{1-\frac{m_f^2}{m_\chi^2}}(m_\chi^2 - m_f^2)\langle v^2\rangle$$
$$\langle\sigma_2 v\rangle = \frac{N_c m_f^2}{16\pi\Lambda^6}\sqrt{1-\frac{m_f^2}{m_\chi^2}}m_\chi^2\left(8+\frac{2m_\chi^2-m_f^2}{m_\chi^2-m_f^2}\langle v^2\rangle\right)$$
$$\langle\sigma_3 v\rangle = \frac{N_c}{48\pi\Lambda^4}\sqrt{1-\frac{m_f^2}{m_\chi^2}} \times\left(24(2m_\chi^2+m_f^2)+\frac{8m_\chi^4-4m_\chi^2m_f^2+5m_f^4}{m_\chi^2-m_f^2}\langle v^2\rangle\right)$$
$$\langle\sigma_4 v\rangle = \frac{N_c}{48\pi\Lambda^4}\sqrt{1-\frac{m_f^2}{m_\chi^2}} \times\left(24m_f^2+\frac{8m_\chi^4-22m_\chi^2m_f^2+17m_f^4}{m_\chi^2-m_f^2}\langle v^2\rangle\right),$$

where v is WIMPs relative velocity in unit c. Specifically, in the early Universe $\langle v^2\rangle \simeq 0.3$, while today $\langle v^2\rangle \simeq 10^{-6}$ (in the following, we use warm DM representing for the former case and cold DM for the latter case). $N_c = 3$ for quark fermion and $N_c = 1$ for lepton fermion. We calculate the limits on Λ for final state of b and u quarks, μ and τ leptons, and for each final state we consider the case of warm DM and cold DM respectively. The corresponding results are shown in Fig. 5. We can find that limits of operators $\mathcal{O}_2$ and $\mathcal{O}_3$ are not sensitive to the relative velocity v.

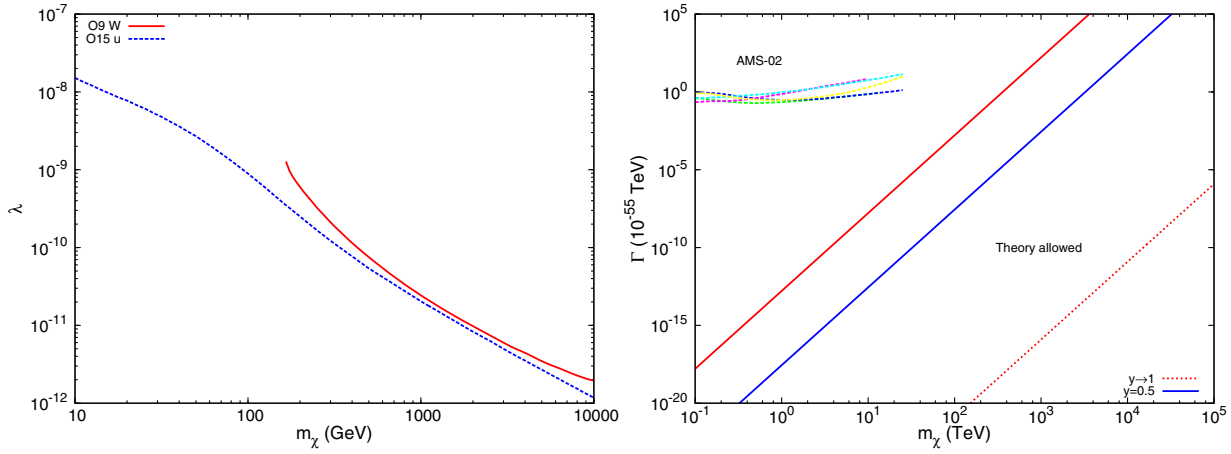

FIG. 6. Left panel: limits on λ as a function of the DM particle mass m_χ at 95% C.L. Right panel: limits on the decay width Γ of interaction $\mathcal{H}_{VA}$ [Eq. (17)] as a function of the DM particle mass m_χ, the region between the red solid line and red dot line is allowed by the theory and the region above the dashed line is excluded by AMS-02.

B. Dark matter decay

As is shown in right panel of Fig. 2, the bound of DM lifetime is $\tau \gtrsim 10^{28}$ s, which indicates that the DM is stable. We can speculate that the decay of WIMPs are suppressed by a very large mass scale such as Planck scale $M_{\rm pl}$. As is pointed out in [83,84] the global symmetries are generically violated at the Planck scale, to describe DM decay they propose some dimension-five effective operators which violate global symmetries. By requiring the couplings $\lambda \sim \mathcal{O}(1)$, they rule out a rather large DM mass range, including the classic WIMP mass range around the electroweak scale. We also use our results to put limits on the coupling of the operators O9 and O15 (see left panel of Fig. 6), our results are similar to [83].

A main characteristic of decay operators proposed in [83] is that the decay final states of a DM only contain SM particles. Herein we consider a decay process in which a DM may decay into another DM and SM particles at the same time, but without taking into account the global symmetries. We consider a V − A effective interaction

$$\mathcal{H}_{\rm VA} = \frac{\lambda^2}{M_{\rm pl}^2}\bar{\varphi}_1\gamma_\mu(1-\gamma_5)\chi_1\bar{\chi}_2\gamma^\mu(1-\gamma_5)\varphi_2, \quad (17)$$

where φ represents a SM particle. It describes the decay process $\chi_1 \to \chi_2\varphi_1\varphi_2$. In the following we assume that SM particles are massless because DM particles masses are always much larger than SM particles. Then the decay width of Eq. (17) is given by

$$\Gamma = \frac{\lambda^4 m_{\chi_1}^5}{96\pi^3 M_{\rm pl}^4}[1 - 8y + 8y^3 - y^4 - 12y^2\ln y], \quad (18)$$

where $y = \frac{m_{\chi_2}}{m_{\chi_1}}$, m_{χ_1} is the mass of DM χ_1 and m_{χ_2} is the mass of DM χ_2. In deriving the decay width, we have assumed that the neutrino (lepton) is the dominant decay channel, for the quark decay channel one should sum over all color states. We also assume that the coupling $\lambda \sim \mathcal{O}(1)$. To ensure the possibility of the decay process $\chi_1 \to \chi_2\varphi_1\varphi_2$ we require that the DM particle χ_2 should be lighter than DM particle χ_1 i.e. $y < 1$. Then to have a solution for Eq. (18), we should also require

$$\frac{96\pi^3 M_{\rm pl}^4\Gamma}{\lambda^4 m_{\chi_1}^5} \lesssim \mathcal{O}(1). \quad (19)$$

This condition is presented in the right panel of Fig. 6 (solid red line). We also calculate the decay width Γ for $y \to 1$ and $y = 0.5$, results are shown by the dot red line and solid blue line in right panel of Fig. 6. The theory allowed region is between the red solid and red dot line, and we can find that the limits on DM lifetime given by AMS-02 experiments are located in the region where the DM parameters room has already been excluded.

V. SUMMARY

In this work, we derive limits on dark matter annihilation cross section and lifetime using measurements of the AMS-02 antiproton ratio and positron fraction data. In deriving the limits, we consider the scenario of secondary particles accelerated in SNR, which can explain the AMS-02 positron fraction and antiproton data at the same time. Then we parametrize the contribution of SNR and calculate the BKG ratio of positron and antiproton by using GALPROP, then we add the SNR component to the BKG component as the total ratio at TOA. We use the likelihood ratio test to determine the significance of a possible DM contribution to the antiproton ratio and positron fraction measured by AMS-02. Upper limits at the 95% C.L. on DM annihilation or decay rate are derived by increasing the signal normalization from its best-fit value of background model, in this way we get the exclusion regions of DM parameters, including the annihilation cross section and lifetime for the final states $b\bar{b}$, $u\bar{u}$, W^+W^- $\mu^+\mu^-$ and $\tau^+\tau^-$ as a function of m_χ, respectively. Specifically, positron fraction is used to calculate the constraints on the annihilation cross section and lifetime for the final states $\mu^+\mu^-$ and $\tau^+\tau^-$ while antiproton ratio is used to calculate the constraints on the annihilation cross section and lifetime for the final states $b\bar{b}$, $u\bar{u}$ and W^+W^-. Under the assumption taken in this work, we find that our limits are stronger than the limits given by Ackermann *et al.* [43] which derived from the Fermi-LAT gamma-ray Pass 8 data observation on the dwarf spheroidal satellite galaxies.

We also consider the uncertainty in our results and find that the propagation parameters contribute most uncertainty at large DM mass (above ∼100 GeV) while the most uncertainty at low DM mass is contributed from solar modulation. As a result, the uncertainty of the limits on the DM parameters is about ∼20%–30% in the whole DM mass range if we take into account the contributions of propagation parameters and solar modulation, this value rises to ∼40%–50% if the contributions of DM distribution profile is considered.

Using these results, we also put limits on the suppression scale Λ of effective field theory as a function of the DM particle mass m_χ for DM annihilation, and we also propose an effective interaction operator which may account for the stability of DM.

ACKNOWLEDGMENTS

We thank the anonymous referee for helpful comments and suggestions. This work is supported by the National Natural Science Foundation of China (under Grants No. 11275097, No. 11475085, and No. 11535005).

[1] J. H. Oort, BAIN **6**, 249 (1932).
[2] F. Zwicky, Astrophys. J. **86**, 217 (1937).
[3] V. C. Rubin and W. K. J. Ford, Astrophys. J. **159**, 379 (1970).
[4] V. C. Rubin, W. K. J. Ford, and N. Thonnard, Astrophys. J. **238**, 471 (1980).
[5] A. Refregier, Annu. Rev. Astron. Astrophys. **41**, 645 (2003).
[6] R. Massey *et al.*, Nature (London) **445**, 286 (2007).
[7] B. W. Lee and S. Weinberg, Phys. Rev. Lett. **39**, 165 (1977).
[8] P. Hut, Phys. Lett. **69B**, 85 (1977).
[9] K. Griest and M. Kamionkowski, Phys. Rep. **333–334**, 167 (2000).
[10] G. Bertonea, D. Hooper, and J. Silk, Phys. Rep. **409**, 279390 (2005).
[11] M. Klasen, M. Pohl, and G. Sigl, Prog. Part. Nucl. Phys. **85**, 1 (2015).
[12] J. Chang *et al.* (ATIC Collaboration), Nature (London) **456**, 362 (2008).
[13] O. Adriani *et al.* (PAMELA Collaboration), Nature (London) **458**, 607 (2009).
[14] O. Adriani *et al.* (PAMELA Collaboration), Phys. Rev. Lett. **106**, 201101 (2011).
[15] M. Aguilar *et al.* (AMS Collaboration), Phys. Rev. Lett. **110**, 141102 (2013).
[16] M. Aguilar *et al.* (AMS Collaboration), Phys. Rev. Lett. **113**, 121101 (2014).
[17] M. Aguilar *et al.* (AMS Collaboration), Phys. Rev. Lett. **113**, 121102 (2014).
[18] M. Aguilar *et al.* (AMS Collaboration), Phys. Rev. Lett. **113**, 221102 (2014).
[19] Y. Z. Fan, B. Zhang, and J. Chang, Int. J. Mod. Phys. D **19**, 2011 (2010).
[20] O. Adriani *et al.* (PAMELA Collaboration), Phys. Rev. Lett. **105**, 121101 (2010).
[21] M. Ackermann, M. Ajello, W. B. Atwood *et al.*, Astrophys. J. **750**, 3 (2012).
[22] Q. Yuan, X. J. Bi, G. M. Chen, Y. Q. Guo, S. J. Lin, and X. M. Zhang, Astropart. Phys. **60**, 1 (2015).
[23] K. Belotsky, M. Khlopov, and M. Laletin, Bled Workshops in Physics **5**, 1 (2014).
[24] L. Feng, Q. Yuan, X. Li, and Y. Z. Fan, Phys. Lett. B **720**, 1 (2013).
[25] P. S. Bhupal Dev, D. K. Ghosh, N. Okada, and I. Saha, Phys. Rev. D **89**, 095001 (2014).
[26] L. Feng, R. Z. Yang, H. N. He, T. K. Dong, Y. Z. Fan, and J. Chang, Phys. Lett. B **728**, 250 (2014).
[27] I. Cholis and D. Hooper, Phys. Rev. D **88**, 023013 (2013).
[28] P. Blasi, Phys. Rev. Lett. **103**, 051104 (2009).
[29] P. Blasi and P. D. Serpico, Phys. Rev. Lett. **103**, 081103 (2009).
[30] P. Mertsch and S. Sarkar, Phys. Rev. Lett. **103**, 081104 (2009).
[31] P. Mertsch and S. Sarkar, Phys. Rev. D **90**, 061301 (2014).
[32] N. Tomassetti, Phys. Rev. D **92**, 081301(R) (2015).
[33] N. Tomassetti, Phys. Rev. D **92**, 063001 (2015).
[34] K. Kohri, K. Ioka, Y. Fujita, and R. Yamazaki, Prog. Theor. Exp. Phys. (2016) 021E01.
[35] X. Li, Z. Q. Shen, B. Q. Lu, T. K. Dong, Y. Z. Fan, L. Feng, S. M. Liu, and J. Chang, Phys. Lett. B **749**, 267 (2015).
[36] L. Bergström, T. Bringmann, I. Cholis, D. Hooper, and C. Weniger, Phys. Rev. Lett. **111**, 171101 (2013).
[37] B. Q. Lu and H. S. Zong, Phys. Rev. D **92**, 103002 (2015).
[38] A. Ibarra, A. S. Lamperstorfer, and J. Silk, Phys. Rev. D **89**, 063539 (2014).
[39] AMS-02 Collaboration, "AMS Days at CERN" and Latest Results, 2015.
[40] G. Giesen, M. Boudaud, Y. Génolini, V. Poulin, M. Cirelli, P. Salati, and P. D. Serpico, J. Cosmol. Astropart. Phys. 09 (2015) 023.
[41] R. Kappl, A. Reinert, and M. W. Winkler, J. Cosmol. Astropart. Phys. 10 (2015) 034.
[42] http://galprop.stanford.edu/.
[43] M. Ackermann *et al.* (The Fermi LAT Collaboration), Phys. Rev. Lett. **115**, 231301 (2015).
[44] W. I. Axford, Ann. N.Y. Acad. Sci. **375**, 297 (1981).
[45] J. C. Higdon and R. E. Lingenfelter, Adv. Space Res. **37**, 1913 (2006).
[46] M. Kafatos and V. A. Fairfax, M. D. Greenbelt, in *Proceedings of 17th International Cosmic Ray Conference, Paris*, Vol. 2 (ICRC, 1981), p. 222.
[47] M. Cassé and J. A. Paul, Astrophys. J. **258**, 860 (1982).
[48] A. Lukasiak, P. Ferrando, F. B. McDonald, and W. R. Webber, Astrophys. J. **426**, 366 (1994).
[49] J. J. Connell and J. A. Simpson, in *Proceedings of 25th International Cosmic Ray Conference, Durban*, Vol. 3 (ICRC, 1997), p. 381.
[50] W. R. Binns *et al.*, AIP Conf. Proc. **598**, 257 (2001).
[51] W. R. Binns *et al.*, Astrophys. J. **634**, 351 (2005).
[52] W. R. Binns *et al.*, New Astron. Rev. **52**, 427 (2008).
[53] M. Cassé and A. Soutoul, Astrophys. J. **200**, L75 (1975).
[54] M. E. Wiedenbeck *et al.*, Astrophys. J. **523**, L61 (1999).
[55] J. C. Higdon, R. E. Lingenfelter, and R. Ramaty, Astrophys. J. **509**, L33 (1998).
[56] Y. Butt, Nature (London) **460**, 701 (2009).
[57] T. K. Gaisser, *Cosmic Rays and Particle Physics* (Cambridge University Press, Cambridge/New York, 1990).
[58] P. D. Serpico, Phys. Rev. D **79**, 021302(R) (2009).
[59] S. J. Lin, Q. Yuan, and X. J. Bi, Phys. Rev. D **91**, 063508 (2015).
[60] M. Di Mauro, F. Donato, N. Fornengo, R. Lineros, and A. Vittino, J. Cosmol. Astropart. Phys. 04 (2014) 006.
[61] E. G. Berezhko, L. T. Ksenofontov, V. S. Ptuskin, V. N. Zirakashvili, and H. J. Völk, Astron. Astrophys. **410**, 189 (2003).
[62] I. Cholis and D. Hooper, Phys. Rev. D **89**, 043013 (2014).
[63] A. W. Strong and I. V. Moskalenko, Astrophys. J. **509**, 212 (1998).
[64] A. W. Strong, I. V. Moskalenko, and V. S. Ptuskin, Annu. Rev. Nucl. Part. Sci. **57**, 285 (2007).
[65] V. N. Zirakashvili, D. Breitschwerdt, V. S. Ptuskin, and H. J. Völk, Astron. Astrophys. **311**, 113 (1996).
[66] O. Adriani *et al.* (PAMELA Collaboration), Astrophys. J. **791**, 93 (2014).
[67] H. S. Ahn *et al.* (CREAM Collaboration), Astropart. Phys. **30**, 133 (2008).
[68] A. Ibarra, D. Tran, and C. Weniger, Int. J. Mod. Phys. A **28**, 1330040 (2013).

[69] T. Sjöstrand, S. Mrenna, and P. Skands, J. High Energy Phys. 5 (2006) 26.
[70] J. F. Navarro, C. S. Frenk, and Simon D. M. White, Astrophys. J. **490**, 493 (1997).
[71] P. Salucci, F. Nesti, G. Gentile, and C. F. Martins, Astron. Astrophys. **523**, A83 (2010).
[72] P. Salucci, arXiv:1008.4344.
[73] D. N. Spergel and P. J. Steinhardt, Phys. Rev. Lett. **84**, 3760 (2000).
[74] W. A. Rolke, A. M. Lopez, and J. Conrad, Nucl. Instrum. Methods Phys. Res., Sect. A **551**, 493 (2005).
[75] G. Steigman, B. Dasgupta, and J. F. Beacom, Phys. Rev. D **86**, 023506 (2012).
[76] J. M. Clem, D. P. Clements, J. Esposito, P. Evenson, D. Huber, J. L'Heureux, P. Meyer, and C. Constantin, Astrophys. J. **464**, 507 (1996).
[77] L. A. Fisk, M. A. Forman, and W. I. Axford, J. Geophys. Res. **78**, 995 (1973).
[78] J. Goodman, M. Ibe, A. Rajaraman, W. Shepherd, Tim M. P. Tait, and H. B. Yu, Phys. Rev. D **82**, 116010 (2010).
[79] Y. Bai, P. J. Fox, and R. Harnik, J. High Energy Phys. 12 (2010) 048.
[80] G. Aad *et al.* (ATLAS Collaboration), Phys. Rev. Lett. **112**, 041802 (2014).
[81] G. Aad *et al.* (ATLAS Collaboration), Eur. Phys. J. C **75**, 92 (2015).
[82] G. Aad *et al.* (ATLAS Collaboration), Phys. Rev. D **91**, 012008 (2015).
[83] Y. Mambrini, S. Profumo, and F. S. Queiroz, arXiv:1508.06635.
[84] M. S. Boucenna, R. A. Lineros, and J. W. F. Valle, Front. Phys. **1**, 34 (2013).